Tree Physiology Advance Access published September 30, 2015

Tree Physiology 00, 1–11
doi:10.1093/treephys/tpv095

Research paper

Dynamics of leaf gas exchange, chlorophyll fluorescence and stem diameter changes during freezing and thawing of Scots pine seedlings

Lauri Lindfors[1,2,3], Teemu Hölttä[1], Anna Lintunen[1], Albert Porcar-Castell[1], Eero Nikinmaa[1] and Eija Juurola[1,2]

[1]Department of Forest Sciences, University of Helsinki, PO Box 27, FI-00014 Helsinki, Finland; [2]Department of Physics, University of Helsinki, PO Box 64, FI-00014 Helsinki, Finland; [3]Corresponding author (lauri.lindfors@helsinki.fi)

Received January 11, 2015; accepted August 17, 2015; handling Editor Marilyn Ball

Boreal trees experience repeated freeze–thaw cycles annually. While freezing has been extensively studied in trees, the dynamic responses occurring during the freezing and thawing remain poorly understood. At freezing and thawing, rapid changes take place in the water relations of living cells in needles and in stem. While freezing is mostly limited to extracellular spaces, living cells dehydrate, shrink and their osmotic concentration increases. We studied how the freezing–thawing dynamics reflected on leaf gas exchange, chlorophyll fluorescence and xylem and living bark diameter changes of Scots pine (*Pinus sylvestris* L.) saplings in controlled experiments. Photosynthetic rate quickly declined following ice nucleation and extracellular freezing in xylem and needles, almost parallel to a rapid shrinking of xylem diameter, while that of living bark followed with a slightly longer delay. While xylem and living bark diameters responded well to decreasing temperature and water potential of ice, the relationship was less consistent in the case of increasing temperature. Xylem showed strong temporal swelling at thawing suggesting water movement from bark. After thawing xylem diameter recovered to a pre-freezing level but living bark remained shrunk. We found that freezing affected photosynthesis at multiple levels. The distinct dynamics of photosynthetic rate and stomatal conductance reveals that the decreased photosynthetic rate reflects impaired dark reactions rather than stomatal closure. Freezing also inhibited the capacity of the light reactions to dissipate excess energy as heat, via non-photochemical quenching, whereas photochemical quenching of excitation energy decreased gradually with temperature in agreement with the gas exchange data.

Keywords: extracellular freezing, living cells, phloem, stomatal conductance, water potential, xylem.

Introduction

The ability of plants to photosynthesize is restricted by low temperatures in winter. This has been studied both in field (Schaberg et al. 1995, Schwarz et al. 1997, Strand et al. 2002) and in controlled freezing experiments (Strand and Öquist 1985, Gaumont-Guay et al. 2003). Most tree species are able to avoid ice nucleation to some extent by supercooling (Wisniewski et al. 2014) to a few degrees below 0 °C (Burke et al. 1976). Temperature measurements in trees have been widely applied to detect the timing and the temperature at which ice nucleation occurs and freezing begins based on detecting the exothermic reaction (Weiser 1970, Burke et al. 1976, Pramsohler et al. 2012). In the exothermic reaction, thermal energy is released due to the phase change of water into ice that can be seen as an increase in temperature, e.g., in temperature measurements inside the stem. In contrast, the thawing moment can be identified based on absorption of energy by water in the endothermic reaction (Silk et al. 1986).

Water relations in trees are profoundly affected by freezing. Many tree species apply an extracellular freezing strategy (Burke

© The Author 2015. Published by Oxford University Press. All rights reserved. For Permissions, please email: journals.permissions@oup.com

Downloaded from http://treephys.oxfordjournals.org/ at University of Helsinki on October 12, 2015

et al. 1976) in which extracellular water freezes while lethal intracellular freezing is avoided due to an increase in osmotic concentration of cell sap. Ice has very low water potential and therefore extracellular freezing creates initially a steep water potential gradient between extracellular ice and cell sap. Water potential of ice decreases 1.2 MPa per 1 °C decrease in temperature (Rajashekar and Burke 1982). Because water always moves towards lower water potential through a semipermeable membrane, living cells experience a net loss of water to the extracellular ice, and dehydrate. Osmotic concentration increases and the volume of living cells decreases with decreasing water content.

Diameter change measurements of the xylem (Irvine and Grace 1997) and living bark constituted of phloem and vascular cambium (Mencuccini et al. 2013) have been used to study changes in the water content of these tissues (Sevanto et al. 2011). Freezing of stem has also been shown to cause reversible shrinkage of xylem and living bark. In the case of living bark this has been interpreted as dehydration and shrinking of living cells (Zweifel and Häsler 2000, Ameglio et al. 2001). Changes in the negative hydrostatic pressure of the xylem and in the positive turgor pressure of the living bark may also be derived from the diameter change measurements provided that the pressure–volume relations of the tissues are known (De Schepper and Steppe 2010). A linear relationship between these two, based on Hooke's law, has been applied to both the xylem (Irvine and Grace 1997) and the living bark (Mencuccini et al. 2013). However, elasticity of living cells can change as a function of their water content (De Schepper and Steppe 2010), complicating the interpretation of the diameter change measurements.

Previous studies have shown that tree water status has large influence on leaf transpiration and photosynthesis during the growing season (Nobel 2009). In evergreen needles, mesophyll cells experience similar freezing-associated water stress as the living cells of stem, which is seen as mesophyll cell shrinkage (Roden et al. 2009). Stem and needles are hydraulically connected through xylem and therefore an ice front and water potential can propagate rapidly within the plant (Pramsohler et al. 2012), although on a study on *Pinus radiata* (D.Don) only little water exchange was observed inside and outside of needle endodermis (Roden et al. 2009).

Several factors related to water stress may contribute to depression of photosynthesis during freezing in addition to the direct effect of temperature. Depression may result from decreased stomatal conductance with lowering water potential. The depression may also occur due to non-stomatal reasons such as biochemical limitations in the Calvin–Benson cycle (Strand and Öquist 1985), decrease in the diffusion rate of carbon dioxide (CO_2) into mesophyll cells due to formation of ice into extracellular spaces (Larcher 1994, Neuner and Pramsohler 2006) and changes in mesophyll conductance of CO_2.

Previous studies on leaf gas exchange have found evidence for the biochemical limitation to photosynthesis at freezing. Intracellular CO_2 concentration (c_i) of foliage has been found to increase following freezing, suggesting that changes in c_i are dominated by decreasing CO_2 consumption by the photosynthetic Calvin–Benson reactions and not so much by decreasing the CO_2 input via the stomata, i.e., stomatal closure (Strand and Öquist 1985, Strand et al. 2002, Gaumont-Guay et al. 2003). The rise in c_i has been suggested to occur due to decreased activity and regeneration capacity of ribulose-1,5-bisphosphate (Strand and Öquist 1985) in the Calvin–Benson cycle.

Although it is well-known that photosynthesis is restricted by low temperatures, photosynthetic rate has not been studied with continuous and high time-resolution leaf gas exchange measurements throughout the process of freezing and thawing in controlled experiments. It is also not well understood how the rapid and profound changes in water potential that take place in mesophyll cells during freezing and thawing affect photosynthesis. Our aim was to characterize the dynamics of the freezing- and thawing-related changes in leaf gas exchange, chlorophyll fluorescence and stem diameter. This was achieved by measuring leaf gas exchange and pulse-amplitude modulated (PAM) chlorophyll fluorescence in parallel with stem diameter changes during a controlled freeze–thaw cycle. To assess how the profound changes in water potential due to freezing and thawing in trees affect photosynthesis, we first studied how freezing and thawing affect living cells in the stem. Following the earlier studies (Zweifel and Häsler 2000, Ameglio et al. 2001) stem diameter dynamics were used as a proxy for water potential changes and they were analysed to assess to what extent they can be explained with the theory of extracellular freezing and dehydration of living cells. Because both the living cells in the inner bark and the mesophyll cells in the leaves experience similar changes in water potential during freezing and thawing, we assumed that mesophyll cells would show approximately similar dynamics in water status as living cells in the inner bark. The changes in water potential can be expected to be similar because water potential of extracellular ice is very low and depends on temperature that is approximately the same in both the stem and the leaves and because water always moves towards a lower water potential through a semipermeable membrane until water potential of cell sap reaches equilibrium with ice. However, the time lags and amplitudes between these two tissues could vary due to the possibly different membrane permeabilities to water, different elastic properties of the cells and different osmotic concentrations before freezing.

Materials and methods

Experimental setup

The effect of the freeze–thaw cycle was studied in Scots pine (*Pinus sylvestris* L.) seedlings in eight identical experiments. The seedlings originated from three different geographical sources: Heinola (61°09′N 26°10′E), Lieksa (63°17′N 30°44′E) and

Downloaded from http://treephys.oxfordjournals.org/ at University of Helsinki on October 12, 2015

Suomenniemi (61°20′N 27°05′E). The seedlings from each origin were 4-year-old crafted clones. The seedlings were overwintered in large pots outdoors at Viikki campus of Helsinki University.

The experiments were done between 4 April and 22 April in 2009, when the seedlings were undergoing spring recovery of photosynthetic capacity. In March, temperature fluctuated between −15 and 6 °C and the weather was mostly sunny. From 30 March, the mean daily temperature stayed continuously above 0 °C. The mostly clear sky weather continued also in April while the temperature was higher, fluctuating between −2 and 12 °C.

Before the start of each experiment, seedlings were placed in a growth chamber (+5 °C, 200 μmol m^{-2} s^{-1}, 9/15 h light/dark period) for 2 days. After this, the seedlings were transferred to an environmental test chamber (WK11—340/40, Weiss Umwelttechnik, Vienna, Austria) with adjustable temperature, where measurement instrumentation was set up. The environmental test chamber was fitted with four LED lights (Ledino, Philips Electronics N.V., P.R.C.) with light intensity of fairly low 200 μmol m^{-2} s^{-1} to avoid photo oxidative damage. Light intensity was verified with a PAR Sensor (Li-190 Quantum sensor, LI-COR Inc., Lincoln NE, USA).

Each experiment consisted of three phase programs; (i) overnight stabilization period in the environmental test chamber; (ii) freeze–thaw cycle; and (iii) 14-h recovery period (Figure 1). Hereafter 'cooling phase' refers to the first half of the freeze–thaw cycle where temperature decreased and 'warming phase' refers to the second half when temperature increased. One full experiment took ~35 h from the instalment in the environmental test chamber until the end of the recovery phase.

During the overnight stabilization period the seedlings were kept in the dark at +5 °C. After the overnight stabilization period, the freeze–thaw cycle was started in the morning 2 h after the lights were switched on. After the onset of the freeze–thaw cycle, temperature was decreased at a rate of 4 °C h^{-1} until −8 °C where temperature was kept steady for 1 h. After that, temperature was increased by 4 °C h^{-1} until it reached again +5 °C. The seedlings remained in the chamber at +5 °C with lights on for the recovery period of 14 h.

Temperature measurements

Needle, xylem and soil temperature was followed with thermocouples (Copper-constantine, T-type). The needle thermocouple was placed between a pair of needles. The xylem thermocouple was placed into a tiny hole ~8 mm deep inside the stem made with an injection needle ~7 cm below diameter change sensors (see below). Temperature inside the environmental test chamber and inside the gas exchange system cuvette (see below) was also measured with radiation-shielded thermocouples.

Diameter change measurements

Stem diameter changes were measured with two pen-like linear variable displacement transducers (LVDT; model AX/5.0/S, Solartron, West Sussex, UK). One sensor head was placed directly on xylem after bark had been removed from a small cross-sectional area surrounding the LVDT head. Another sensor was placed on the living bark after the dead outer bark had been removed from a small cross-sectional area surrounding the LVDT head. The living bark refers to the layer of phloem and vascular cambium, although relative diameter change from vascular cambium is insignificantly small due to its small cross section. The measurements were conducted before the active growth started so that there was no newly formed xylem and phloem tissue. Diameter change of the living bark was calculated by subtracting

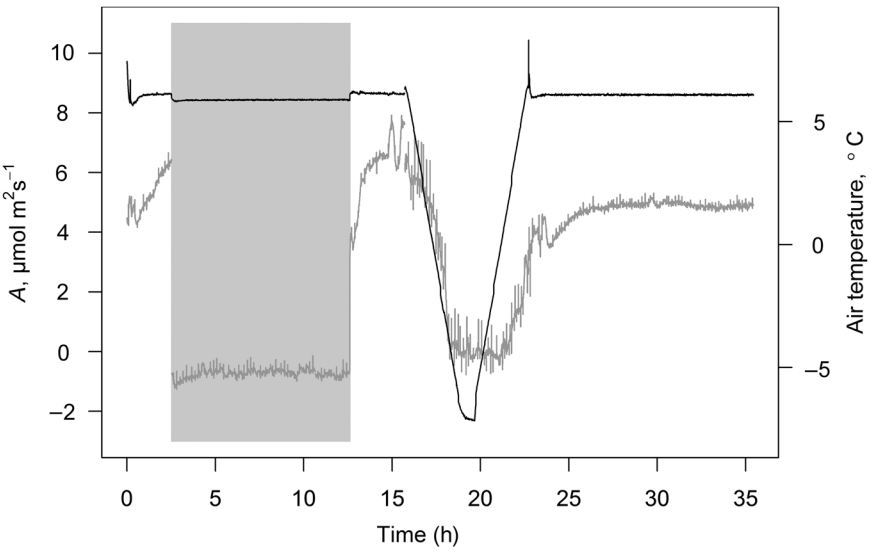

Figure 1. Example of conditions inside the environmental test chamber during an experiment. Air temperature (black line) and CO_2 assimilation (*A*, grey line) were measured by a GFS-3000 measuring head inside the environmental test chamber. Total photosynthetic photon flux density (PPFD) was 200 μmol m^2 s^{-1}, except for a dark period during the stabilization phase when PPFD was zero (grey area).

Downloaded from http://treephys.oxfordjournals.org/ at University of Helsinki on October 12, 2015

the diameter change measured on xylem from the diameter change measured on the living bark. The LDTV sensors were installed ~10 cm above the base of the seedling's stem (diameter ~1.5 cm). The sensors were fixed on the stem by attaching the sensors first on a brass bar that was fixed on the stem with aluminium frames attached to both ends of the bar, enclosing both the bar and the stem inside opposite sides of the frames. Data from the thermocouples and LVDT were stored with a datalogger. Measuring interval was 10 s during the freeze–thaw cycle and 60 s during the rest of the experiments.

Gas exchange and chlorophyll fluorescence measurements

A photosynthetic gas exchange measuring system coupled to a standard cuvette (Walz GFS-3000, Heinz Walz GmbH, Effeltrich, Germany) was used to measure continuously CO_2 and H_2O exchange from which assimilation (A), transpiration (E), stomatal conductance (g_s) and intracellular CO_2 concentration (c_i) from needles were estimated in addition to measurement of cuvette CO_2 concentration (c_a) during the experiments. Four needle pairs were placed into the cuvette. Cuvette temperature was set to follow the conditions inside the environmental test chamber and cuvette light intensity was set to 200 µmol m^{-2} s^{-1}. Air for the gas exchange system was taken from outdoors and was completely dried during the freeze–thaw treatment to avoid condensation of water inside the measurement system during the experiment at low temperatures. Outdoor ambient CO_2 concentration was used and it varied between 353 and 518 ppm. Before the start of the freeze–thaw cycle, the relative humidity inside the cuvette was 10–13% and during the freeze–thaw cycle it was below 3%. The measuring frequency was 1 s, and data were stored as 5-s averages every 20 s.

The maximum quantum yield of PSII (F_v/F_m) was measured in the seedlings in the field to ascertain the background level of photosynthetic down-regulation prior to the experiments. We estimated the maximum quantum yield of PSII in needles dark-acclimated for 2 h with a portable fluorometer (FMS-2, Hansatech Ltd, Norfolk, UK) using the saturating light pulse technique to calculate the fluorescence parameter F_V/F_M (Maxwell and Johnson 2000), where variable fluorescence F_V, is the difference between maximal fluorescence F_M (obtained during the saturating pulse), and minimal fluorescence F_0 (obtained after dark acclimation in the dark).

Fluorescence measurements were also carried out during the experiments to follow the dynamics of fluorescence at time t (F_t), the operating quantum yield of PSII (ΦP), as well as the non-photochemical (NPQ) and photochemical (PQ) quenching parameters in the needles in response to the freeze–thaw cycle (Maxwell and Johnson 2000, Porcar-Castell et al. 2014). Measurements were conducted with a monitoring PAM fluorometer (Heinz Walz GmbH) (Porcar-Castell et al. 2008*b*). The purpose of this measurement was to assess the effects of freezing on photosynthesis with an independent measurement carried out in a different set of needles, and to examine the response of the light reactions to the freeze–thaw cycle. Statistical analysis was conducted with Wilcoxon signed rank test.

Results

Freeze–thaw dynamics

Ice nucleation occurred in needles on average at –4.3 °C (standard deviation (SD) = 0.26) and in xylem at –3.9 °C (SD = 0.25), indicated by an exothermic reaction and a rapid increase in temperature (see Figure 2). The rapid increase in temperature is characteristic for freezing of supercooled liquid. The difference in ice nucleation temperature was statistically significant ($P < 0.05$). Water potential of ice equivalent to the ice nucleation temperature is –5.2 MPa for needles and –4.7 MPa for xylem. However, due to the sudden rise, temperature in xylem soon reached –1.0 °C, that is only –1.2 MPa in terms of water potential of ice. The rise in temperature during the exotherm could not be reliably determined in the case of needles due to low tissue mass. In contrast, cooling rate was lower for xylem due to higher mass of tissue. Temperature of soil remained above zero throughout the experiments. We also observed that the rate of temperature decrease temporarily slowed down during an 'exotherm event' that followed approximately half an hour after ice nucleation (see Figure 2). Thawing began in xylem when temperature reached on average –0.04 °C (SD = 0.22).

Dynamics of xylem and living bark diameter

Both stem and living bark diameters reacted rapidly to ice nucleation during the cooling phase of the freeze–thaw cycle (Figure 3a (point 1) and b). Living bark diameter reacted always

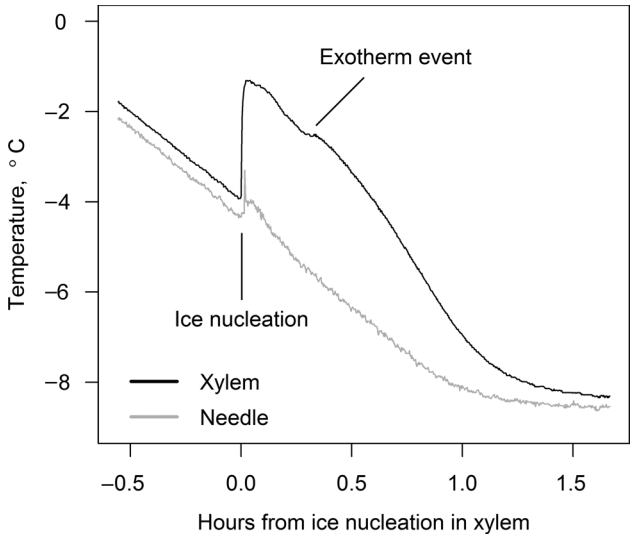

Figure 2. An example of temperature and interpretation of its dynamics in various parts of seedling during an experiment.

Downloaded from http://treephys.oxfordjournals.org/ at University of Helsinki on October 12, 2015

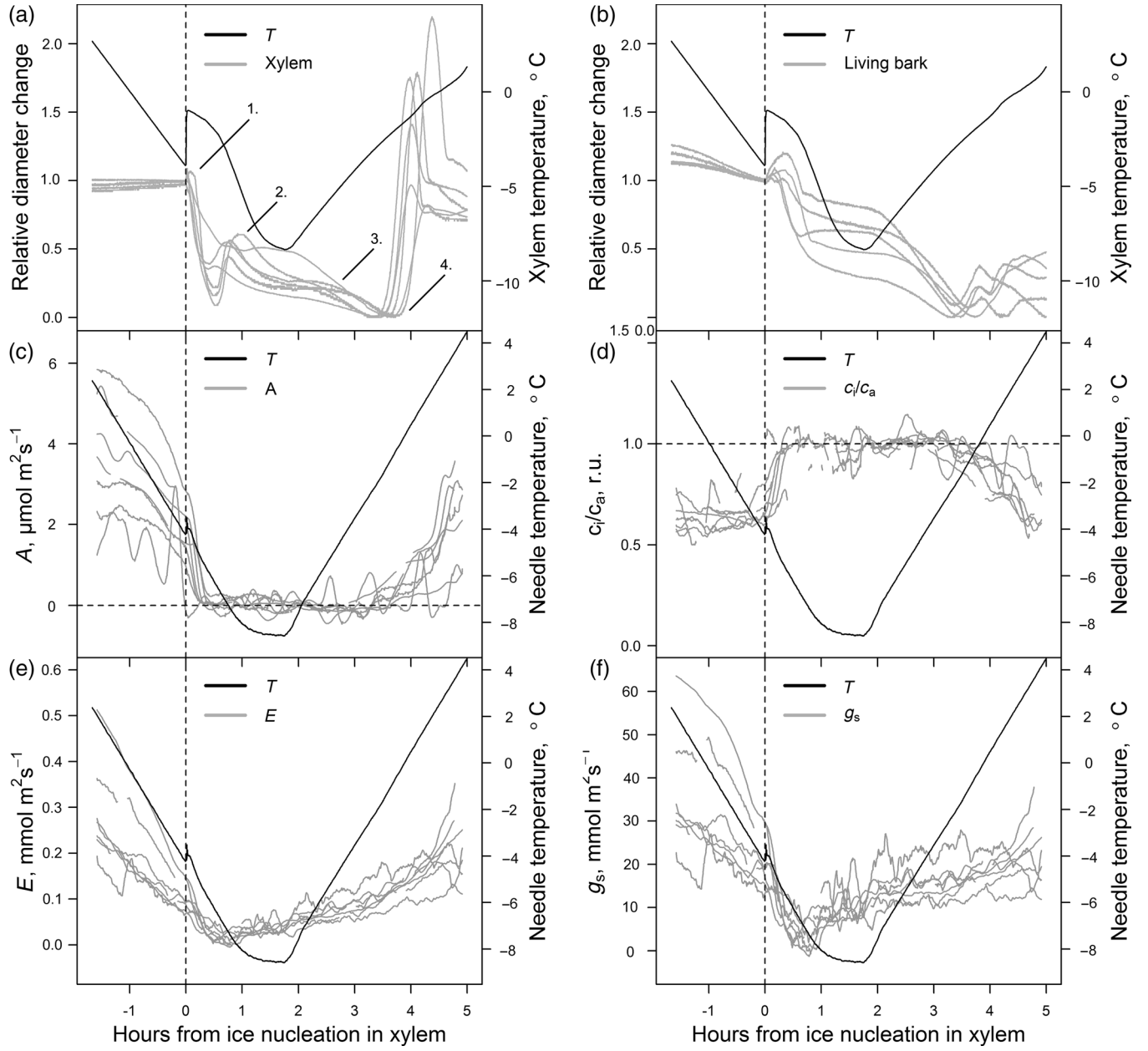

Figure 3. Dynamics of temperature and gas exchange parameters in needles and diameter changes of xylem and living bark during the freeze–thaw cycle. Gas exchange parameters CO_2 assimilation (c), intracellular CO_2 concentration (c_i) divided by ambient CO_2 concentration (c_a) (d), transpiration (e) and stomatal conductance (f) are running averages of 31 points within an interval of 10 min and 18 s. *N* for the parameters was between 5 and 7. Vertical dashed line refers to the moment of ice nucleation in xylem. Horizontal dashed line refers to the zero (c) or to the '1.0' value of the left *y*-axis (d). Black solid line in (a and b) is xylem temperature and in (c–f) it is needle temperature. The temperature curves are means of data from the seven experiments and *N* for other parameters in the figures is between 5 and 7. Diameter changes (a and b) are normalized to the value at the moment of ice nucleation in xylem (value = '1') and are scaled so that the value '0' represents the minimum value during each experiment. Numbers in (a) refer to events in xylem diameter; (1) first temporary expansion and/or beginning of much larger shrinking; (2) second temporary expansion; (3) increase in shrinking rate; and (4) rapid expansion and new maximum diameter.

with small and temporary expansion prior to shrinking, whereas that happened in xylem only in half of all experiments. Xylem expanded 0.048% (SD = 0.023) of initial thickness, i.e., 5.1 µm (SD = 4.3) and living bark 0. 24% (SD = 1.3) of initial thickness, i.e., 18 µm (SD = 13).

The shrinking of xylem and living bark followed soon after ice nucleation in all experiments (Figure 3a (point 1) and b). Xylem shrank 0.56% (SD = 0.30) of initial thickness, i.e., 64 µm (SD = 46) and living bark 13% (SD = 5.4) of initial thickness, i.e., 160 µm (SD = 48). Also, a second temporary expansion (Figure 3a (point 2)) occurred during the shrinking in xylem but not in living bark diameter. Interestingly, diameters continued to shrink even long after air and xylem temperatures had begun to increase during the warming phase of the freeze–thaw cycle.

Downloaded from http://treephys.oxfordjournals.org/ at University of Helsinki on October 12, 2015

The rate of shrinking even slightly increased when temperature began to rise (Figure 3a (point 3)).

During the warming phase of the freeze–thaw cycle, xylem diameter expanded rapidly to a new maximum, followed by a decline to the level that was close to the initial diameter before the start of the freeze–thaw cycle (Figure 3a (point 4)). This phenomenon was absent from the living bark diameter, which stayed low even after the thawing of the xylem (Figure 3b).

Dynamics of photosynthesis

During the cooling phase, gas exchange reacted to both decrease in temperature and ice nucleation. A clear decrease in CO_2 assimilation rate (A) was observed due to the decreasing temperature already before ice nucleation (Figure 3c). However, in all experiments A dropped rapidly to almost zero after ice nucleation in stem/needles. A remained very low thereafter, until the needle temperature had reached ~0 °C during the warming phase of the freeze–thaw cycle.

Stomatal conductance (g_s) followed a similar pattern as A during the cooling phase, but the drop induced by the ice nucleation was not as drastic (Figure 3c and f). Transpiration (E) had a distinct trend relative to A and g_s (Figure 3c, e and f). A fell to 10% of initial value in ~17 min after ice nucleation in xylem whereas g_s fell in ~45 min before reaching its minimum value during the freeze–thaw cycle. Difference in dynamics between the three variables was characteristic after the drop and during the warming phase. E did not stabilize during the course of the freeze–thaw cycles (see Figure 3e). Furthermore, E and g_s started to increase gradually already before the minimum temperature was reached.

Intracellular CO_2 concentration (c_i) started to rise following the ice nucleation (Figure 3d), and rose close to the ambient level. c_i began to fall more gradually in the warming phase of the freeze–thaw cycle after temperature had reached ~0 °C parallel to the increase of CO_2 exchange rate.

In addition to gas exchange properties, we tracked the dynamics of fluorescence over time F_t, of the operating quantum yield of PSII (ΦP), as well as those of PQ and NPQ processes (Figure 4). The ΦP decreased with decreasing temperatures and slightly increased during the recovery phase. Photochemical quenching showed a similar pattern to that of ΦP. Non-photochemical quenching increased with decreasing temperatures but the decrease was suddenly inhibited after the freezing took place. Subsequently, this inhibition was released during the recovery phase and NPQ continued to increase in most of the runs. F_t decreased or remained constant along with decreasing temperature until the ice nucleation in the stem (Figure 4a). After ice nucleation, however, F_t started to increase in most experiments and reached its maximum approximately at the time when a minimum ambient temperature was reached, starting to

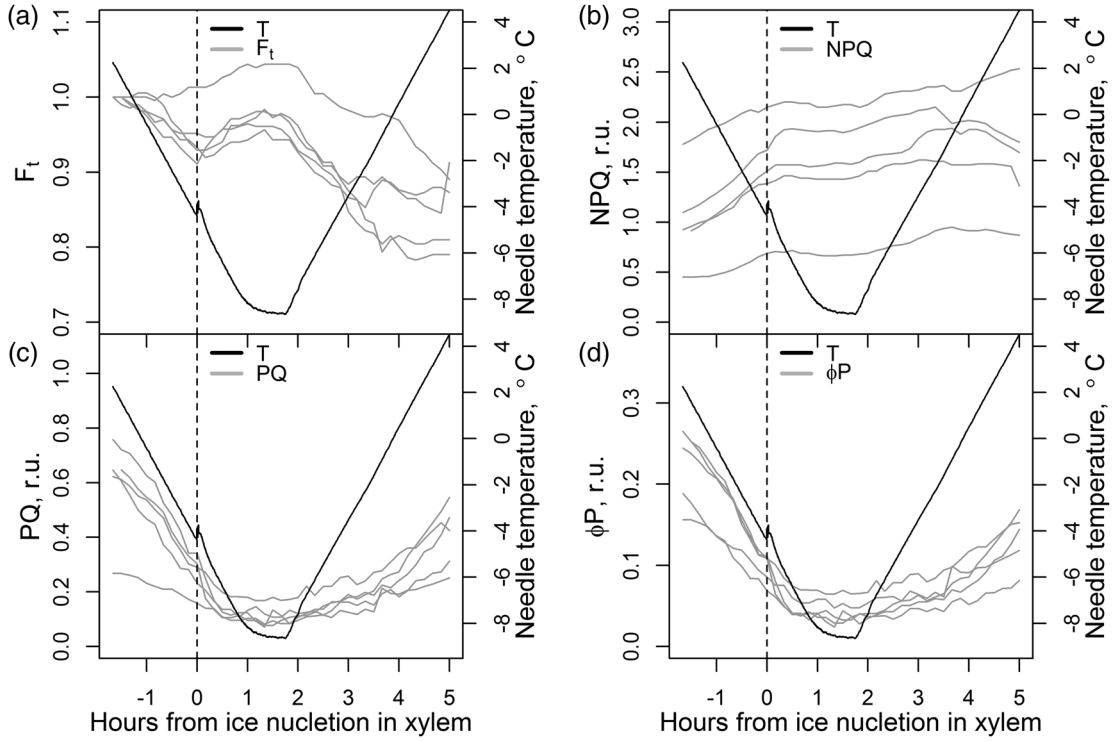

Figure 4. Dynamics of fluorescence at time t (a), non-photochemical quenching (b), photochemical quenching (c) and operating quantum yield of photosystem II (d) during the freeze–thaw cycle. Vertical dashed line refers to the moment of ice nucleation in xylem. Fluorescence at time t (F_t) was normalized to the value when PPFD was zero, obtained prior to the start of the freeze–thaw cycle, for each experiment (a). The temperature curves are means of data from the seven experiments.

Downloaded from http://treephys.oxfordjournals.org/ at University of Helsinki on October 12, 2015

decline again when temperature started to increase. At the end of the freeze–thaw cycle F_t was, on average ~11% lower compared with the value at the moment of ice nucleation.

The initial level of the maximum quantum yield of PSII (F_v/F_m), ascertained prior to each experiments, varied between 0.71 and 0.83.

Differences in gas exchange and diameter change dynamics

We analysed the temporal relationship between gas exchange and diameter change with respect to freezing and thawing in more detail to reveal the possible sequence in the processes and to relate the different phenomena to each other (Figure 5).

Diameter changes were the first parameter to react to ice nucleation in xylem with temporary expansion (Figure 5a). The drop in A and g_s usually occurred before the start of the shrinking in xylem and A fell close to zero before the shrinking began in living bark. The second temporary expansion in xylem began on average ~5 min after the shrinking in living bark. The exotherm event in xylem followed the second temporary expansion in xylem on average ~10 min later.

Parallel to the moment at which air temperature began to increase during the freeze–thaw cycles, a change in the rate of diameter change could be seen in xylem and living bark (Figure 5b). A began to gradually increase after air temperature had approximately reached 0 °C. Parallel to the start of the gradual increase of A, xylem diameter began to expand rapidly and temporarily peaked ~50 min later to a maximum diameter in the course of the whole experiment. When thawing occurred in xylem A had already increased to 40% of the value at the moment of ice nucleation in xylem. No rapid changes in the dynamics of E and g_s could be seen during the warming phase of the freeze–thaw cycle.

We also compared the values of leaf gas exchange and xylem and living bark diameters at the end of each experiment with their values before the freeze–thaw cycle (see Table 1). Carbon dioxide assimilation rate decreased from before the freeze–thaw cycle by ~30%. Xylem diameter returned to almost its preceding value while diameter of the living bark did not recover so well.

Discussion

We characterized here the dynamics in leaf gas exchange, chlorophyll fluorescence and stem diameter changes in Scots pine seedlings in conditions where they experienced profound and sudden changes in water relations due to freezing and thawing. We showed that rapid shrinking of xylem and living bark occurred parallel to an exothermic reaction in xylem, indicating that freezing was taking place. The shrinking of living bark has been explained to be caused by dehydration and shrinking of living cells following extracellular freezing (Zweifel and Häsler 2000, Ameglio et al. 2001). Parallel to the events in the stem we also observed depression of photosynthesis.

Freeze–thaw cycle

We observed clear patterns in CO_2 assimilation and transpiration during the freeze–thaw cycle, whereas the dynamics were more complicated in diameter change and in fluorescence signal. The late spring status of the seedlings ensured high enough signal in the measurements, yet they were still winter hardened so that the experiment did not injure the seedlings. Late spring status of seedlings was ascertained with measurement of F_V/F_M before the experiments and was between 0.71 and 0.83, which is lower compared with values of 0.86–0.88 obtained with the same instrument and protocol in pine needles during summer (Porcar-Castell et al. 2008*a*). The rate of temperature decrease was such that no physical damage was observed after the

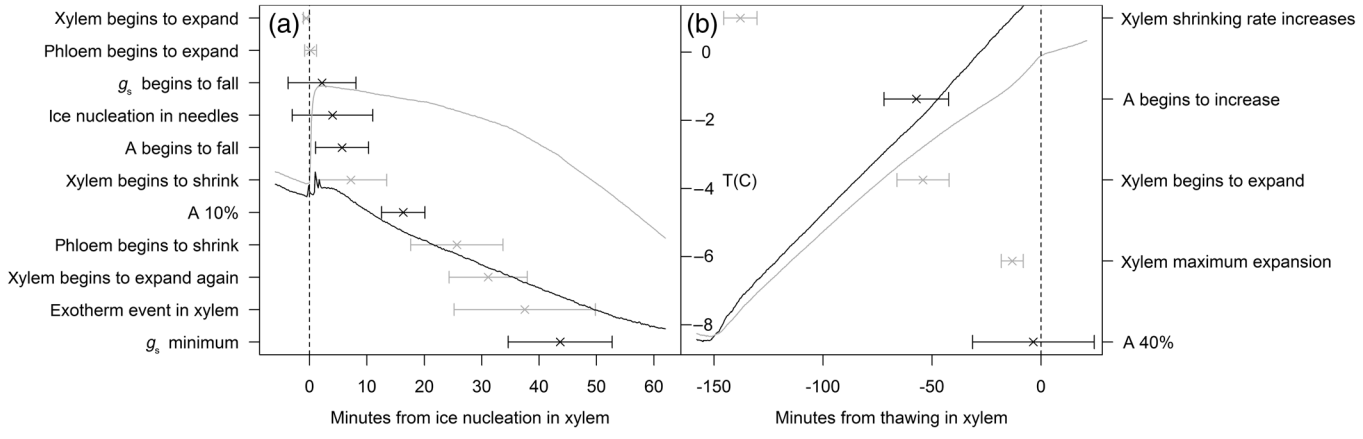

Figure 5. Dynamics of phenomena related to stem (grey solid lines and grey horizontal bars) and to needles (black solid lines and black horizontal bars) following ice nucleation (a) and thawing (b) in xylem. The zero on the *x*-axis and the vertical dashed line refer to the moment of ice nucleation (a) and thawing (b) in xylem. Cross marks refer to the average timing (±SD) of the phenomena that are explained on the side *y*-axis. See also Supplementary Data at *Tree Physiology* Online for an explanation of how data were analysed. The temperature curves are means of data from the seven experiments.

Downloaded from http://treephys.oxfordjournals.org/ at University of Helsinki on October 12, 2015

Table 1. The change in parameters from the beginning of the freeze–thaw cycle to the end of the experiment as the average value of all repetitions of the experiment. A is the CO_2 assimilation rate, E is the transpiration rate, g_s is the stomatal conductance and c_i is the intracellular CO_2 concentration. Standard deviation was 1.6–1.5 for A, 0.1 for E, 13–17 for g_s, 27–28 for c_i, 35 for phloem diameter change and 17 for xylem diameter change. *$P < 0.05$, **$P < 0.01$.

Parameters	Beginning of freeze–thaw cycle	End of experiment	Relative change	Absolute change
A, µmol m^2 s^{-1}	4.01	2.64	0.67	1.37**
E, mmol m^2 s^{-1}	0.322	0.221	0.71	0.101**
g_s, mmol m^2 s^{-1}	39.1	26.6	0.71	12.5**
c_i, ppm	290	259	0.90	31*
Xylem diameter change, µm				−13.0*
Living bark diameter change, µm				−61.3**

freeze–thaw cycle, photosynthesis recovered to on average 67% of the value before the freeze–thaw cycle by the end of the experiments (Table 1). However, the diameter of the living bark remained decreased by the end of the experiments. Permanent shrinking of living bark diameter has been suggested to be caused by freezing damage to living cells in the stem (Améglio et al. 2003).

The effect of freezing on the stem diameter

Freezing propagated rapidly throughout the whole tree as has also been shown in previous studies (Kitaura 1967, Hacker and Neuner 2007, Pramsohler et al. 2012). Freezing of xylem occurred on average 6 s after freezing of living bark and freezing of needles occurred on average 33 s after freezing of xylem.

Generally the xylem and living bark diameter dynamics were in agreement with the theory of shrinking of stem diameter due to dehydration of living cells (Zweifel and Häsler 2000, Ameglio et al. 2001). The diameters shrink with decreasing temperature. While the relationship between temperature and water potential of ice is linear, decrease of water content of living cells can decrease their elasticity (Murphy and Ortega 1995), which can explain some of the nonlinear behaviour seen in the living bark diameter changes. Furthermore, movement of water through the plasma membrane can be slow and occur with a time lag, especially as viscosity of water increases with decreasing temperature (Haynes 2012).

The slowness of the water movement may be seen in Figure 3a (point 3) and b. While air temperature already began to increase after the minimum temperature of the freeze–thaw cycle, the shrinking rates of xylem and living bark even increased. It may be that due to slow movement of water through the plasma membrane, living cells did not reach equilibrium hydraulically with the extracellular ice, even though the minimum temperature of the treatment was reached. Therefore, after the temperature began to increase during the warming phase, water movement through the plasma membrane became more rapid as viscosity of water decreases with rising temperature.

In addition to the shrinking of living bark, we observed also a considerable shrinking in xylem diameter. However, shrinking of living bark diameter was on average 20-fold higher than shrinking of xylem diameter when compared with initial thickness of those tissues. While xylem consists mostly of dead tracheid cells, xylem still holds a considerable amount of parenchyma cells (Spicer 2014) that contribute to the shrinking.

Some other dynamics in the diameter changes were more difficult to explain with the theory of shrinking of living cells alone. Diameter reacted to ice nucleation with temporary expansion in living bark and also in half of experiments in xylem (see Figure 3a (point 1)). Also a second temporary expansion could be seen ahead of the exotherm event in xylem (see Figure 3a (point 2)). The expansions could be related to increase in gas or liquid pressure inside the stem due to lower specific density of ice compared with liquid water (Robson and Petty 1987). Roden et al. (2009) observed ice formation in tracheids of vascular bundles of *P. radiata* needles that expanded into the space formerly occupied by shrinking living cells. Temporary swelling of xylem could then result from rapid ice formation in xylem tracheid followed by more gradual shrinking of living cells that is slowed down by membrane permeability and increasing viscosity.

The 'exotherm event' that was observed in temperature in which the rate of temperature change temporarily increases has been explained by the freezing of water that is moving out from living cells during their dehydration and has even been considered as a separate freezing event (Weiser 1970). Instead of being a completely separate freezing event the phenomena described as the 'exotherm event' may be a point where freezing temporarily intensifies during a continuous process of freeing. We found that the exotherm event began after living bark and xylem diameters had already begun to shrink. Some other process may have caused the diameter to shrink before the exotherm event such as the gas release from the stem (Lintunen et al. 2014). On the other hand, other possible explanations for the exotherm event could be freezing of water under high tension in low diameter pores in cell walls (Ashworth and Abeles 1984) or freezing of water with high osmotic concentration, and the xylem and bark shrinking could reflect dehydration of living cells as suggested above.

During the warming phase, living bark and xylem diameters followed interesting dynamics. Living bark did not recover back to its diameter before ice nucleation and xylem diameter began to recover back only ~2 h after the onset of the warming phase (see Figure 3a and b). Increase in temperature and water potential of ice during the warming phase likely caused the water potential gradient between ice and living cells to reverse as water potential of ice became higher than water potential of living cells. This leads to net uptake of water by living cells.

Downloaded from http://treephys.oxfordjournals.org/ at University of Helsinki on October 12, 2015

The large reversible expansion in xylem diameter during thawing (see Figure 3a (point 4)) may be related to radial water movement between living bark and xylem (Zweifel and Häsler 2000). It seems likely that the outer layer of the stem, i.e., the living bark, thawed ahead of xylem as air temperature gradually increased during the warming phase of the freeze–thaw cycle. Therefore, a steep water-potential gradient could have developed between ice in xylem and liquid water in living bark, resulting in movement of water from living bark to xylem. Afterwards, the xylem diameter decreases back to the level before freezing of xylem, but living bark did not recover to its initial diameter.

Effect of freezing on photosynthesis

Photosynthetic rate decreased in the cooling phase of the freeze–thaw cycle already before ice nucleation (Figure 3c), which could be explained by, e.g., temperature dependency of photosynthesis or mesophyll conductance, or by the gradually decreasing stomatal conductance (Figure 3f). The operating quantum yield of photochemistry (ΦP), the fluorescence at time t (F_t) and the PQ parameter all decreased with decreasing temperature, reflecting the temperature-dependent decrease in energy utilization by the Calvin–Benson reactions (Figure 4). As expected, thermal energy dissipation in PSII was enhanced in response to decreasing temperature via the regulation of NPQ to compensate for the decreasing photochemical utilization of excitation energy.

Interestingly, we observed the temperature-inhibition of the NPQ regulatory mechanisms at the moment of freezing (Figure 4b), which restricted the further accumulation of NPQ. The enzymatic inhibition of Violazanthin de-epoxidize, the enzyme responsible for the main process behind NPQ, at low temperatures is well-known (e.g., Eskling et al. 1997). This phenomenon was also observed in F_t, which changed from a decreasing trend to an increasing trend at the moment of freezing. Because both PQ and NPQ compete for excitation energy with fluorescence, a decrease in PQ at constant NPQ results in an increase in F_t (Porcar-Castell et al. 2008*a*). Also in previous studies, a significant increase in the basic fluorescence (F_0) has been detected in leaves after freezing (Neuner and Pramsohler 2006, Hacker et al. 2008). During the thawing phase, the tendency in F_t was again reversed as the temperature inhibition in NPQ was released and PQ started to increase.

The fact that both A and F_t responded simultaneously to the freezing suggests that intracellular freezing affects photosynthesis at multiple scales. In addition, the simultaneous decrease in operating quantum efficiency of PSII (ΦP) and in A measured in different needles upon freezing corroborates that the sudden decrease in A was not the result of any measurement artifact.

Leaf gas exchange may have also been affected by freezing of water inside leaves due to extracellular freezing (Larcher 1994, Neuner and Pramsohler 2006). The extracellular ice efficiently fills the intracellular spaces (Roden et al. 2009). The diffusion coefficient of CO_2 in ice is many orders of magnitude lower in comparison with that in liquid water. It does not seem likely that the path of CO_2 into the mesophyll cells would have been completely blocked, given that A fell close to zero in ~17 min. Therefore, it is perhaps unlikely that an increase in the resistance of CO_2 diffusion due to ice formed at the time of ice nucleation would be the only reason for the depression of photosynthesis.

CO_2 assimilation rate (A) and stomatal conductance (g_s) had very distinct dynamics after ice nucleation (see Figure 3c and f). Both the A and the g_s had a declining trend before ice nucleation but in both cases the decline rate increased after it. Only a brief stomatal closure occurred ~45 min after ice nucleation, but after that g_s started to increase steadily, although slowly, even when the temperature still continued to drop. A remained stable at zero until temperature increased above 0 °C, even though g_s had already long before that reached approximately the level it had before ice nucleation. The transpiration rate, however, did not reach a similar stable state. The asymmetry in dynamics between A and g_s and only the brief closure of the stomata seems to suggest that depression of photosynthesis was not caused primarily by stomatal closure, but trees rather seemed to lose some of their ability for stomatal control.

Another indication for this is that the calculated internal CO_2 concentration increased close to the ambient level during the frozen period, which could be expected if the stomata were open and there was no photosynthesis. The increase in intracellular CO_2 concentration during freezing has been observed also in previous studies (Strand and Öquist 1985, Gaumont-Guay et al. 2003).

The dynamics of stomatal conductance may at least partly be explained by the so called hydropassive mechanism, where dehydration of epidermal cells pull the guard cells of stomata apart forcing the stomata open (Buckley 2005). The loss of stomatal control in cold conditions is not very detrimental to trees as vapour pressure deficit in cold conditions is never very large. Also freezing of water in needles may prevent excessive water loss from needles. We hypothesize that the increase in c_i may also follow from decrease in mesophyll conductance for CO_2, further preventing the consumption of CO_2 in photosynthesis. Mesophyll conductance can decrease along with increasing viscosity of cell sap as water content decreases when mesophyll cells dehydrate. Viscosity and the diffusion coefficient of CO_2 are inversely related (Juurola et al. 2005). Decreasing temperature further increases viscosity (Thompson 2006) and decreases CO_2 diffusion rate (Aalto and Juurola 2002) in cell sap. On the other hand, decrease in volume of mesophyll cells can increase the CO_2 diffusion rate as transport distances decrease.

Comparing dynamics in photosynthesis and stem diameter change

The diameter change of living bark was generally in agreement with the theory of extracellular freezing of living cells (Zweifel

Downloaded from http://treephys.oxfordjournals.org/ at University of Helsinki on October 12, 2015

and Häsler 2000, Ameglio et al. 2001) and its rapid shrinkage may therefore reflect how living cells in general experience the profound changes in water relations caused by extracellular freezing. Water in extracellular spaces inevitably freezes and creates steep water potential between ice and sap of the living cells. Water always moves towards a lower water potential through a semipermeable membrane, which affects the water content and the volume of living cells.

However, the permeability of plasma membrane and elastic properties of the cell wall, and osmotic concentration can be different for the living bark and the other living cells (Nobel 2009) and therefore the amplitude and the time lags for volume changes can be different. It is also possible that some axial movement of water occurred between stem and needles due to the different time dynamics of freezing. Water tensions may develop between different parts of tree due to water potential gradient if the different parts freeze or thaw at different times. However, in the case of leaves of *P. radiata* it was found that endoderm surrounding the vascular bundle in needles may hinder water movement between xylem and mesophyll cells (Roden et al. 2009). Also, temperature increased less due to the exothermic reaction in needles than in the stem and therefore mesophyll cells may have experienced even more extreme freezing-related dehydration than the living cells in the stem.

Depression of photosynthesis after ice nucleation occurred parallel to the shrinking in xylem and in living bark on a similar temporal scale (Figure 3a–c). The photosynthetic rate had fallen after ice nucleation to 10% of its rate before ice nucleation of needles in ~17 min. Time constant for volumetric changes in mesophyll can be estimated to be even smaller than this (Nobel 2009). Similar timescales of the rapid changes in gas exchange and in the diameter of living bark supports the argument that mesophyll cells may have experienced rapid dehydration comparable to living cells in the living bark.

Stomata remained partially open throughout the freezing–thawing cycle, which may lead to plant water loss, particularly at thawing, as the permanent shrinking of bark tissue suggests. The latter could also indicate tissue damage in the bark (Roden et al. 2009) although the saplings were still partly winter-acclimated during the experiment. The plant water loss could lead to needle dehydration as often reported for conifers (Mayr et al. 2002) if various freeze–thaw cycles are repeated, particularly in the spring when the abundant sunlight exposes the needles to high excitation pressure.

During the warming phase of the freeze–thaw cycle, photosynthesis began to recover rapidly after ambient temperature had reached ~0 °C. At that time temperature of xylem was still about −2 °C, which is equivalent to water potential of ice of −2.4 MPa. Photosynthesis began to recover even though there was an apparent water potential gradient persisting between xylem in the stem and needles. On the other hand, water potential of ice of −2.4 MPa is close to minimal values (Martínez-Vilalta et al. 2009) observed during summer in Scots pine, suggesting that the seedlings should have been able to sustain such water potential levels while still photosynthesizing.

Overall, our results show how the dynamics of leaf gas exchange and stem diameter are affected by freezing in trees. Stem diameter changes exhibited complex dynamics that were generally in agreement with the theory of extracellular freezing, reflecting water status changes in living cells. Large and nearly simultaneous changes in the diameters of xylem and living bark suggest that similar low water potentials develop throughout the tree. The diameter dynamics suggest that freezing and low viscosity may have prevented efficient water movement across pressure gradients and rising of temperature is required before mass flow takes place. The dynamics of leaf gas exchange and chlorophyll fluorescence measurements suggest that the photosystem was affected by freezing at multiple levels. While both the CO_2 assimilation rate and stomatal conductance decreased after ice nucleation, the earlier recovery of stomatal conductance before photosynthetic rate and before thawing of needles reveals that the decreased CO_2 assimilation reflects impaired dark reaction rather than stomatal closure. Furthermore, the inhibition of NPQ upon freezing suggests that a concomitant enzymatic inhibition takes place in the photosynthetic light reactions.

Supplementary data

Supplementary data for this article are available at *Tree Physiology* Online.

Conflict of interest

None declared.

Funding

This work was supported by the Academy of Finland (268342 and Centre of Excellence 1118615, 272041); Doctoral Programme in Atmospheric Sciences; ICOS (271878); ICOS-Finland (281255); ICOS-ERIC (281250); a 3-year research grant offered by the University of Helsinki; and the Nordic Centre of Excellence CRAICC.

References

Aalto T, Juurola E (2002) A three-dimensional model of CO_2 transport in airspaces and mesophyll cells of a silver birch leaf. Plant Cell Environ 25:1399–1409.

Ameglio T, Cochard H, Ewers FW (2001) Stem diameter variations and cold hardiness in walnut trees. J Exp Bot 52:2135–2142.

Améglio T, Cochard H, Ewers FW (2003) Gelista™: a new tool for testing frost hardiness by stem diameter variations on walnut. Environ Stress Hortic Crops 618:509–514.

Downloaded from http://treephys.oxfordjournals.org/ at University of Helsinki on October 12, 2015

Ashworth EN, Abeles FB (1984) Freezing behavior of water in small pores and the possible role in the freezing of plant tissues. Plant Physiol 76:201–204.

Buckley TN (2005) The control of stomata by water balance. New Phytol 168:275–292.

Burke MJ, Gusta LV, Quamme HA, Weiser CJ, Li PH (1976) Freezing and injury in plants. Annu Rev Plant Physiol 27:507–528.

De Schepper V, Steppe K (2010) Development and verification of a water and sugar transport model using measured stem diameter variations. J Exp Bot 61:2083–2099.

Eskling M, Arvidsson PO, Åkerlund HE (1997) The xanthophyll cycle, its regulation and components. Physiol Plant 100:806–816.

Gaumont-Guay D, Margolis HA, Bigras FJ, Raulier F (2003) Characterizing the frost sensitivity of black spruce photosynthesis during cold acclimation. Tree Physiol 23:301–311.

Hacker J, Neuner G (2007) Ice propagation in plants visualized at the tissue level by infrared differential thermal analysis (IDTA). Tree Physiol 27:1661–1670.

Hacker J, Spindelböck JP, Neuner G (2008) Mesophyll freezing and effects of freeze dehydration visualized by simultaneous measurement of IDTA and differential imaging chlorophyll fluorescence. Plant Cell Environ 31:1725–1733.

Haynes WM (ed) (2012) CRC handbook of chemistry and physics. CRC Press, Boca Raton, FL.

Irvine J, Grace J (1997) Continuous measurements of water tensions in the xylem of trees based on the elastic properties of wood. Planta 202:455–461.

Juurola E, Aalto T, Thum T, Vesala T, Hari P (2005) Temperature dependence of leaf-level CO_2 fixation: revising biochemical coefficients through analysis of leaf three-dimensional structure. New Phytol 166:205–215.

Kitaura K (1967) Supercooling and ice formation in Mulberry trees. In: Asahina E (ed) Cellular injury and resistance in freezing organisms. Proceedings of International Conference on Low Temperature Science, Vol. 2. Bunyeido Printing Co., Sapporo, pp 143–156.

Larcher W (1994) Photosynthesis as a tool for indicating temperature stress events. In: Schulze ED, Caldwell MM (eds) Ecophysiology of photosynthesis. Ecological Studies 100. Springer, Berlin, pp 261–277.

Lintunen A, Lindfors L, Kolari P, Juurola E, Nikinmaa E, Hölttä T (2014) Bursts of CO_2 released during freezing offer a new perspective on avoidance of winter embolism in trees. Ann Bot 114:1711–1718.

Martínez-Vilalta J, Cochard H, Mencuccini M et al. (2009) Hydraulic adjustment of Scots pine across Europe. New Phytol, 184:353–364.

Maxwell K, Johnson GN (2000) Chlorophyll fluorescence—a practical guide. J Exp Bot 51:659–668.

Mayr S, Wolfschwenger M, Bauer H (2002) Winter-drought induced embolism in Norway spruce (*Picea abies*) at the Alpine timberline. Physiol Plant 115:74–80.

Mencuccini M, Hölttä T, Sevanto S, Nikinmaa E (2013) Concurrent measurements of change in the bark and xylem diameters of trees reveal a phloem-generated turgor signal. New Phytol 198:1143–1154.

Murphy R, Ortega JKE (1995) A new pressure probe method to determine the average volumetric elastic modulus of cells in plant tissue. Plant Physiol 107:995–1005.

Neuner G, Pramsohler M (2006) Freezing and high temperature thresholds of photosystem II compared to ice nucleation, frost and heat damage in evergreen subalpine plants. Physiol Plant 126:196–204.

Nobel PS (2009) Physicochemical and environmental plant physiology. Academic Press, San Diego.

Porcar-Castell A, Juurola E, Nikinmaa E, Berninger F, Ensminger I, Hari P (2008*a*) Seasonal acclimation of photosystem II in *Pinus sylvestris*. I. Estimating the rate constants of sustained thermal energy dissipation and photochemistry. Tree Physiol 28:1475–1482.

Porcar-Castell A, Pfündel E, Korhonen JFJ, Juurola E (2008*b*) A new monitoring PAM fluorometer (MONI-PAM) to study the short- and long-term acclimation of photosystem II in field conditions. Photosynth Res 96:173–179.

Porcar-Castell A, Tyystjärvi E, Atherton J, van der Tol C, Flexas J, Pfundel EE, Moreno J, Frankenberg C, Berry JA (2014) Linking chlorophyll a fluorescence to photosynthesis for remote sensing applications: mechanisms and challenges. J Exp Bot 65:4065–4095.

Pramsohler M, Hacker J, Neuner G (2012) Freezing pattern and frost killing temperature of apple (*Malus domestica*) wood under controlled conditions and in nature. Tree Physiol 32:819–828.

Rajashekar CB, Burke MJ (1982) Liquid water during slow freezing based on cell water relation and limited experimental testing. In: Li PH, Sakai A (eds) Plant cold hardiness and freezing stress–mechanisms and crop implications. Academic Press, New York, pp 211–221.

Robson DJ, Petty JA (1987) Freezing in conifer xylem I. Pressure changes and growth velocity of ice. J Exp Bot 38:1901–1908.

Roden JS, Canny MJ, Huang CX, Ball MC (2009) Frost tolerance and ice formation in *Pinus radiata* needles: ice management by the endodermis and transfusion tissues. Funct Plant Biol 36:180–189.

Schaberg PG, Wilkinson RC, Shane JB, Donnelly JR, Cali PF (1995) Winter photosynthesis of red spruce from three Vermont seed sources. Tree Physiol 15:345–350.

Schwarz PA, Fahey TJ, Dawson TE (1997) Seasonal air and soil temperature effects on photosynthesis in red spruce (*Picea rubens*) saplings. Tree Physiol 17:187–194.

Sevanto S, Hölttä T, Holbrook NM (2011) Effects of the hydraulic coupling between xylem and phloem on diurnal phloem diameter variation. Plant Cell Environ 34:690–703.

Silk WK, Hsiao TC, Diedenhofen U, Matson C (1986) Spatial distributions of potassium, solutes, and their deposition rates in the growth zone of the primary corn root. Plant Physiol 82:853–858.

Spicer R (2014) Symplasmic networks in secondary vascular tissues: parenchyma distribution and activity supporting long-distance transport. J Exp Bot 65:1829–1848.

Strand M, Öquist G (1985) Inhibition of photosynthesis by freezing temperatures and high light levels in cold-acclimated seedlings of Scots Pine (*Pinus sylvestris*). 1. Effects on the light-limited and light-saturated rates of CO_2 assimilation. Physiol Plant 64:425–430.

Strand M, Lundmark T, Söderbergh I, Mellander PE (2002) Impacts of seasonal air and soil temperatures on photosynthesis in Scots pine trees. Tree Physiol 22:839–847.

Thompson MV (2006) Phloem: the long and the short of it. Trends Plant Sci 11:26–32.

Weiser CJ (1970) Cold resistance and injury in woody plants: knowledge of hardy plant adaptations to freezing stress may help us to reduce winter damage. Science 169:1269–1278.

Wisniewski M, Gusta L, Neuner G (2014) Adaptive mechanisms of freeze avoidance in plants: a brief update. Environ Exp Bot 99:133–140.

Zweifel R, Häsler R (2000) Frost-induced reversible shrinkage of bark of mature subalpine conifers. Agric For Meteorol 102:213–222.

Downloaded from http://treephys.oxfordjournals.org/ at University of Helsinki on October 12, 2015